



Exploring the Energy Frontier with Deep Inelastic Scattering at the LHC

A Contribution to the Update of the European Strategy on Particle Physics

LHeC and PERLE Collaboration

contacts: Oliver Brüning (CERN) and Max Klein (U Liverpool)

Executive Summary

The Large Hadron Collider determines the energy frontier of experimental collider physics for the next two decades. The High Luminosity LHC could be further upgraded with a 60 GeV energy, high current electron beam by using novel Energy Recovery Linear Accelerator (ERL) techniques which enable TeV energy scale electron-proton collisions at a 1000 times HERA's luminosity. A joint ECFA/CERN and NuPECC initiative led to a detailed conceptual design report (CDR) [1] for the Large Hadron Electron Collider (LHeC) published in 2012. Since then, the LHC performed in a magic way and the Higgs boson was discovered with no further sign of BSM physics as yet. Based on a mandate of the CERN Directorates and guided by International Advice, this motivated representatives of more than 100 institutes to further evaluate the extension of the experimental base for exploring energy frontier particle physics. They proceeded, as sketched here, with the development of the accelerator, physics and detector prospects for ep and pp twin-collisions at the LHC, with the intention to publish a CDR update in early 2019 [2].

The very high luminosity, achievable through the combination of HL LHC and an electron ERL, and the substantial extension of the kinematic range in deep inelastic scattering (DIS) compared to HERA makes the LHeC a uniquely powerful TeV energy collider, maximally exploiting the LHC infrastructure. Realising an "Electrons for LHC" [3] programme would create the cleanest, high resolution microscope accessible to the world, a '**Hubble Telescope for the Micro Universe**', directed to unravel secrets of the complex dynamics of the strong interaction which the LHC and future hadron colliders also demand. Being complementary to the LHC and a future e^+e^- machine, it would scrutinise the Standard Model (SM) deeper than ever before, and possibly discover new physics in the electroweak and chromodynamic sectors. Adding ep transforms the LHC into an outstanding, high precision Higgs facility at $O(1)$ BSF cost. Through the extension of the kinematic range by about three orders of magnitude in lepton-nucleus scattering, the LHeC is the most powerful electron-ion research facility one can build in the next decades, for resolving the chromodynamic origin of the Quark-Gluon-Plasma, the ridge and determining the unknown partonic substructure and dynamics inside nuclei.

This physics programme goes beyond any specialised goal, it complements and sustains the physics at HL LHC by providing new discovery potential in its final phase of operation. The LHeC represents a unique opportunity for CERN and its associated laboratories to build a full, new machine using modern technology. The ERL has major future applications, with ep at HE LHC, as an injector for FCC-ee, for building the FCC-eh or, beyond particle physics, as the highest energy XFEL of hugely increased brightness [4]. The main LHeC innovation is the first ever high energy application of energy recovery technology, based on high quality superconducting RF developments, a major contribution to the development of *green* collider technology. A novel ep experiment enables modern detection technology, such as HV CMOS Silicon tracking, to be further developed and exploited in a new generation, 4π acceptance, no pile-up, high precision collider detector in the decade(s) hence.

This paper focuses on physics providing also an overview on the machine. It is complemented by an Addendum [5] describing, as required, further aspects of the LHeC project such as the operation and timelines for the accelerator and the detector. The development of multi-turn, high current, 802 MHz ERL technology, required for the LHeC, is described in an accompanying, separate strategy contribution of the PERLE Collaboration [6] on a 500 MeV ERL facility at Orsay, based on its CDR [7] published in 2017.

47 1 Physics

48 1.1 LHeC - the World's Cleanest High Resolution Microscope

49 QCD is a gauge theory of asymptotically free partons, the dynamics of which has to be established ex-
50 perimentally for which deep inelastic scattering (DIS) is the most appropriate means. DIS determines the
51 momentum densities of partons, quarks and gluons, as functions of the negative four-momentum transfer
52 squared, Q^2 , between the scattering electron and proton and of the fraction, x , of the momentum of the par-
53 ent proton carried by the parton. The DIS resolution of substructure is $\propto 1/\sqrt{Q^2}$, where 1 GeV corresponds
54 to resolving distances of 0.2 fm. The LHeC covers an unprecedented range in Q^2 from below 1 GeV² to above
55 a TeV². A salient feature of ep scattering is that one can freely, within the detector acceptances, prescribe
56 Q^2 . Thus the **LHeC represents the cleanest deep microscope of matter the world can build.**

57 In the future, **major alterations of QCD may become manifest** [8], such as the embedding of QCD
58 in a higher gauge theory possibly unifying electroweak and strong interactions or colour may be freely ob-
59 served. Crucial questions of QCD await to be resolved such as the **confinement question**, called one of the
60 millenium puzzles to be explained [9], the possible relation of QCD to string theory and the use of to gravita-
61 tion techniques (AdS-CFT), or the CP violation related to **axions** which may explain dark matter. Principal
62 questions in QCD such as the existence of **instantons**, the reason for the occurrence of diffraction in high en-
63 ergy collisions, **new dynamics at high parton densities** or the precision **test for factorisation** [10] all
64 ought to be answered or/and studied much deeper. Proton structure extends to transverse dimensions, and
65 a new field of research, related to **generalised and unintegrated parton distributions**, is to be explored.
66 Similarly, huge deficits exist in the understanding of the **parton structure of the neutron, the deuteron,**
67 **nuclei, the photon and the Pomeron.** QCD is complex and fundamental and the value of DIS extremely
68 rich, and they shall not be reduced to the sheer question of how well we know the PDFs in the proton.

69 The PDF capability of the LHeC has been studied in detail in the CDR [1] and the status of updating
70 this, which will be completed early 2019, has been presented at length recently [11] including the importance
71 and **the prospect to measure α_s to per mille accuracy in DIS.** The PDF programme of the LHeC is
72 of unprecedented depth for the following reasons:

- 73 • For the first time it will resolve the partonic structure of the proton and nuclei completely, i.e. deter-
74 mine the **$u_v, d_v, u, d, s, c, b, \text{ the top and gluon momentum distributions}$** through neutral
75 (NC) and charged current (CC) cross section and direct heavy quark (s,c,b,t) PDF measurements in
76 a hugely extended kinematic range, from $x = 10^{-6}$ to 0.9 and from Q^2 about 1 to 10^6 GeV².
- 77 • Very high luminosity, an unprecedented precision from new detector technology and through the
78 redundant evaluation of the event kinematics from the lepton and hadron final states will lead to
79 **extremely high PDF precision** and to the determination of the various PDF analysis parameters,
80 such as **m_c** (to 3 MeV), **m_b** (to 10 MeV) and **V_{cs}** (to below 1%), from the data themselves.
- 81 • Because of the high LHeC energy, the weak probes (W, Z), unlike at HERA or the low energy EIC,
82 dominate the interaction at larger Q^2 and resolve the flavours. Thus **no other data will be required:**
83 that is, there is no influence from higher twists or nuclear uncertainties or data inconsistencies, i.e.
84 LHeC will be the unique base for PDFs, independently of the LHC, for predictions, discovery and
85 novel tests of theory¹. This includes a **full understanding of the gluon** which dominates the par-
86 ton dynamics below the valence-quark region and generates the mass of the visible matter.

87 Given the impressive theoretical progress on pQCD, see [12], one will have these PDFs consistently available
88 at N³LO as is required, for example, for the N³LO $pp \rightarrow gg H$ cross-section calculations and **enabling high**
89 **precision SM LHC measurements such as of the Higgs couplings in pp or of $\sin^2(\theta_W)$.** For QCD,
90 this will resolve open issues (and probably creating new ones) on α_s , answer the question on the persistence
91 (or not) of the linear parton evolution equations at small x , see Sect. 1.2, and also decisively test whether
92 factorisation holds or not between DIS and Drell-Yan scattering.

¹This may then be confronted with so-called global PDF analyses based on an inclusive assembly of all possible sources for sensitivity to parton distributions, suffering from sizeable theoretical uncertainties and known and forthcoming difficulties of data compatibility which are hidden through so-called χ^2 tolerance criteria.

93 1.2 Novel Dynamics and Approaches in Quantum Chromodynamics

94 The LHeC offers clean and unique access to very low values of Bjorken- x , where novel QCD phenomena are
95 predicted to occur. It has been known since the seminal work of **Balitskii – Fadin – Kuraev – Lipatov**
96 that there are large logarithms of $\alpha_s \ln 1/x$ which need to be taken into account in the perturbative expansion
97 in QCD, though next-to-leading order terms are large and unstable. Appropriate resummation schemes,
98 combining BFKL and DGLAP dynamics, have been constructed which stabilise the solution. Recent fits
99 that include the resummation of low- x terms within the DGLAP framework [13] show a marked improvement
100 in the description of HERA data at low x and low Q^2 . Such effects will be strongly amplified in the LHeC
101 kinematic range and clarified.

102 Another phenomenon that has been predicted to occur at very low x and low scales is **parton saturation**,
103 where the densely packed gluons start to recombine, slowing down the growth in their density with decreasing
104 x . Simulations demonstrate that when saturation effects are present, standard DGLAP fits fail to
105 describe the simulated LHeC data when F_2 and F_L (or F_2^{cc}), are simultaneously included [1]. Knowledge of
106 QCD dynamics at small x will have severe consequences for future high energy hadron colliders, influencing
107 production rates of heavy particles such as electroweak and Higgs bosons. This can only be resolved with
108 the LHeC in an unambiguous way as it requires high precision DIS data in a kinematic range extended
109 compared to HERA and for Q^2 large enough for ensuring α_s to be small.

110 The LHeC will offer unprecedented capabilities for studying **diffractive processes**, based on either
111 proton tagging or large rapidity gap signatures. As well as the semi-inclusive diffraction DIS process,
112 $ep \rightarrow eYp$ and its eA analogue, exclusive J/Ψ , Υ production and Deeply Virtual Compton scattering can
113 be measured precisely. With the large lever arm in x and Q^2 , diffractive parton densities can be extracted
114 over a wide kinematic domain and used to evaluate diffractive factorisation through their comparisons with
115 diffractive jet and charm rates which was found at HERA to be broken. The deep theoretical relation
116 between diffraction in ep scattering and nuclear shadowing will be explored. Measurements at low Q^2 and
117 of F_L in diffraction will pin down higher twist effects and potentially reveal their relation to saturation.
118 Inclusive eA measurements will permit extractions of diffractive nuclear parton densities for the first time.

119 The large statistics and high t resolution in exclusive channels will allow **generalised parton densities**
120 to be extracted the Fourier transform of which yields the transverse spatial distribution of partons inside the
121 hadron. Through the exclusive diffractive production of di-jets and charmed mesons, the Wigner functions
122 can be extracted, simultaneously characterising the partonic momentum and **transverse spatial structure**,
123 and thus revealing the size of the configurations in the nucleon wave function and offering sensitivity to Gri-
124 bnov diffusion and chiral dynamics. The transverse nucleon gluonic size is an essential ingredient in saturation
125 models and determines the initial conditions of the non-linear QCD evolution equations. The nucleon trans-
126 verse quark and gluon distributions also drive predictions of the underlying event structure in inclusive pp
127 scattering and the rapidity gap survival probability in hard single and central exclusive diffraction.

128 Finally, low- x physics at the LHeC will have a deep impact on **neutrino astronomy**. The ultra-high
129 energy neutrinos that are observed at the IceCube observatory typically interact at very low values of x ,
130 thus requiring large extrapolations relatively to current collider data. Similarly, the production of prompt
131 neutrinos in the heavy meson decays, that dominate high energy atmospheric neutrino fluxes and may also
132 contribute to astrophysical neutrino sources, is mostly determined by low x and low momentum scales, and
133 is thus extremely sensitive to novel QCD dynamics as described above which only the LHeC will unravel.

134 1.3 Discovery through High Precision: Electroweak and Top Physics

135 At the LHeC, precision electroweak physics is performed through measurements of the inclusive neutral-
136 current and charged-current DIS cross sections [16, 17], as well as measurements of more exclusive final
137 states, such as charm or top production in CC DIS or direct production of EW gauge bosons. The measure-
138 ments of inclusive NC and CC DIS cross sections at LHeC and FCC-eh, as displayed in Fig. 1, will extend to
139 significantly higher scales with much larger cross sections than HERA. At the highest scales Q^2 , accessible
140 to the LHeC, up to about 70% of the NC cross section is mediated by Z -boson exchange or γZ -interference
141 terms. These measurements provide **very high precision determinations of the weak neutral current**
142 **couplings of the light quarks**, improving the presently best achieved uncertainties by very large fac-

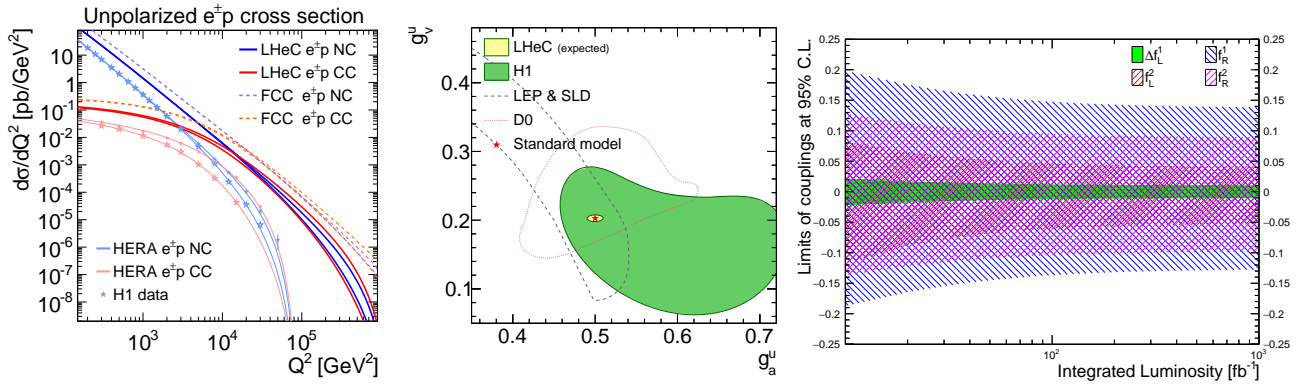


Figure 1: Left: Unpolarised inclusive NC and CC DIS cross sections as a function of Q^2 at the LHeC, in comparison to HERA (H1 [14]) and FCC-eh expectations; Middle: Determination of the up-quark weak neutral current couplings from LEP/SLD, D0, H1 and the LHeC; Right: Expected sensitivities as a function of the integrated luminosity on the SM and anomalous W_{tb} couplings [15].

143 tors [18], see Fig. 1. The quantum nature of the electroweak theory is further tested through unique
 144 measurements in the space-like region of the **scale dependence of the effective weak mixing angle**,
 145 from below the Z pole to about a TeV, with an uncertainty of $\sin^2 \theta_{\text{eff}}^{\ell} \simeq 0.01\%$ [18]. Furthermore, the
 146 ρ -parameter and $\sin^2 \theta_{\text{eff}}$ can be measured with high precision for different quark flavours, and, again, their
 147 scale-dependence is going to be determined for the first time. Noteworthy, these measurements are fully
 148 complementary to ee and pp colliders, which are performed in the time like region. The high precision PDFs
 149 from LHeC permit the total uncertainty on $\sin^2 \theta_W$ at the LHC to be twice better than that at LEP/SLD
 150 as was shown by ATLAS [19].

151 The huge electroweak effects and large e^- polarisation permit to precisely measure novel structure func-
 152 tions, such as $F_2^{\gamma Z}$, and to **access hitherto unknown PDFs**, such as $F_{bb}^{\gamma Z}$, while testing the universality
 153 of the interaction of partons in DIS with photons and Z bosons accurately for the first time. The CC elec-
 154 troweak sector can be uniquely accessed at high scales over many orders of magnitude in Q^2 at the LHeC. This
 155 provides a very precise determination of the **W boson mass with an uncertainty of order 10 MeV** in
 156 ep. Of high importance is the reduction of the PDF related uncertainty on M_W at HL-LHC to below 2 MeV
 157 which promises a $4 \cdot 10^{-5}$ accuracy test of a most crucial electroweak parameter, as estimated by ATLAS [20].
 158 Contrary to former believes, the LHC has become a precision measurement facility. With ep added it may
 159 see the SM fail.

160 Due to the much increased cms energy compared to HERA, the LHeC represents a **novel top quark**
 161 **factory**, with a total single t cross section of 1.9 (4.5) pb in ep at HL (HE) LHC [15]. The other important
 162 top-quark production mode is $t\bar{t}$ photo-production [21]. The high luminosity and the cleanliness of the final
 163 state make top quark physics in DIS an attractive and competitive research area for the first time. This
 164 includes high precision electroweak top quark measurements and sensitive searches for new physics.

165 One **flagship measurement is the direct measurement of the CKM matrix element V_{tb}** to 1%
 166 at just 100 fb^{-1} , which is a determination free of any model assumptions such as on the unitarity of the CKM
 167 matrix or the number of quark generations. LHeC has an **outstanding search potential for anomalous**
 168 **top quark couplings**: left-handed (L), and right-handed (R) W_{tb} vector (1) and tensor (2) couplings
 169 $f_{L,R}^{1,2}$ [15]. In the SM $f_L^1 = 1$ (with $f_L^1 \equiv 1 + \Delta f_L^1$), and $f_R^1 = f_L^2 = f_R^2 = 0$. Based on hadronic top
 170 quark decays only, the expected accuracies for these couplings as a function of the integrated luminosity are
 171 presented in Fig. 1 (right). Anomalous admixtures to the SM coupling f_L^1 can be measured at the 1% level
 172 already at 100 fb^{-1} , while anomalous contributions to the other couplings can be traced down to order 5%.
 173 Similarly, the CKM matrix elements $|V_{tx}|$ ($x = d, s$) can be extracted through the analysis of W boson and
 174 bottom (light) quark associated production channels, where the W boson and b -jet (light jet) final states
 175 can be produced via s-channel single top quark decay or t-channel top quark exchange [22].

176 Single top quark CC production can also be used to search for **Flavour Changing Neutral Currents**
 177 (FCNC) $tu\gamma$, $tc\gamma$, tuZ , and tcZ couplings with high sensitivity [23], see below. In top-quark pair production

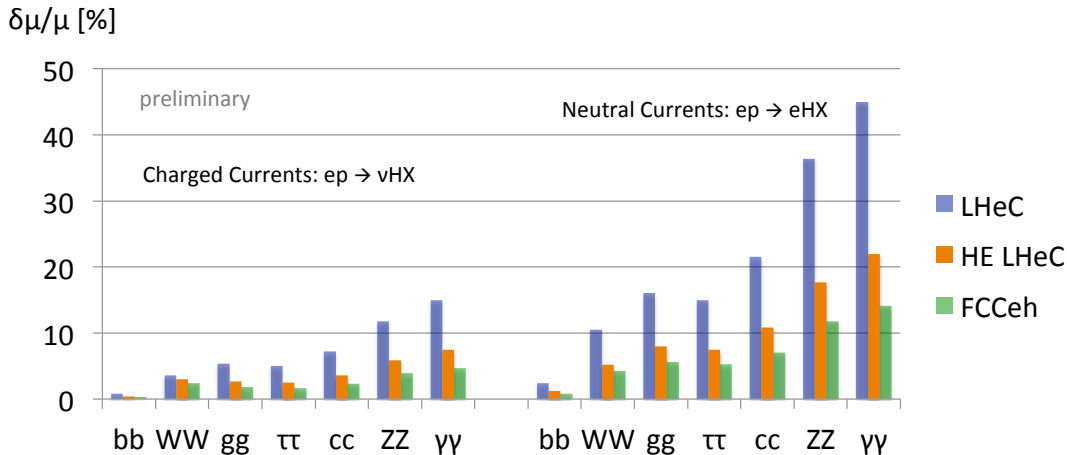


Figure 2: Uncertainties of signal strength determinations in the seven most abundant SM Higgs decay channels for the FCC-eh (green, 2 ab^{-1}), the HE LHeC (brown, 2 ab^{-1}) and LHeC (blue, 1 ab^{-1}), in charged and neutral current DIS production.

178 sensitive searches for anomalous $t\bar{t}\gamma$ and $t\bar{t}Z$ chromoelectric and chromomagnetic dipole moments in $t\bar{t}$
 179 production can be performed leading to expected accuracies down to the 5% level [21].

180 Other exciting results of top quark properties and promising **searches for BSM physics in the top**
 181 **quark sector** involve, for example, the first time investigation of the top quark structure function inside
 182 the proton, the study of top quark spin and polarization in DIS, the analysis of the CP-nature in $t\bar{t}H$
 183 production, and a sensitive search for anomalous FCNC tHq couplings.

184 1.4 Higgs: Precision Measurements and Exotics

185 The deep exploration of the Higgs mechanism and its possible relation to physics beyond the SM, for decades
 186 ahead, will be the central theme of the HL LHC and of all new energy frontier colliders under discussion.
 187 Owing to the intense LHC proton beams, the LHeC has a special role in this endeavour, mainly because ep
 188 transforms the LHC into a precision Higgs facility at moderate cost. The main Higgs production mechanism
 189 at LHeC is charged current deep inelastic scattering, $ep \rightarrow H\nu X$. The Higgs production CC (NC) DIS cross
 190 section in LO QCD is $\sigma \simeq 190$ (26) fb. The Higgs boson in ep is thus dominantly produced via WW fusion,
 191 with a total event sample of $2 \cdot 10^5$ Higgs bosons, nearly 60% of which in the SM are decaying into $b\bar{b}$. Each
 192 decay, of significant branching, is simultaneously measured in $ZZ \rightarrow H$ production. Uniquely, CC and NC
 193 production are distinguished and the final state, with a pile-up of 0.1, permits for a clean reconstruction of
 194 a Higgs boson, which is rather centrally produced, and its decay.

195 The analysis of SM Higgs decays in ep, summarised in [24], has been performed in two major steps:
 196 First, very detailed simulations and signal extraction studies, BDT and independently cut based, were made
 197 for the dominant $H \rightarrow b\bar{b}$ and the challenging $H \rightarrow c\bar{c}$ channels. Second, prospects were evaluated for
 198 the seven most frequent decay channels both in NC and CC, in which acceptances and backgrounds were
 199 estimated with Madgraph, and efficiencies, distinguishing leptonic and hadronic decay channels for W , Z ,
 200 and τ , were taken from prospective studies on Higgs coupling measurements at the LHC [25]. This provided
 201 an uncertainty estimate, comprising the signal-to-background ratio, acceptance and reconstruction efficiency
 202 effects, on the signal strength μ_i for each of the Higgs decay channels i . This method was benchmarked
 203 with the detailed simulations for charm and beauty decays mentioned above.

204 Fig. 2 shows the estimated signal strength uncertainties for the 7 most frequent Higgs decay channels,
 205 measured in CC and NC, as expected for the LHeC, ep with HE-LHC and the FCC-eh. With the joint CC
 206 and NC measurements one constrains seven scaling parameters in the so-called κ formalism in a redundant
 207 way. The joint measurement of NC and CC Higgs decays provides nine constraints on κ_W and nine on
 208 κ_Z together with two each for the five other decay channels considered. Since the dominating channel of
 209 $H \rightarrow b\bar{b}$ is precisely determined, there follows **a precise determination of the κ values**, especially for
 210 the vector boson and b couplings, as is shown in Fig. 3. A feature worth noting is the “transfer” of precision

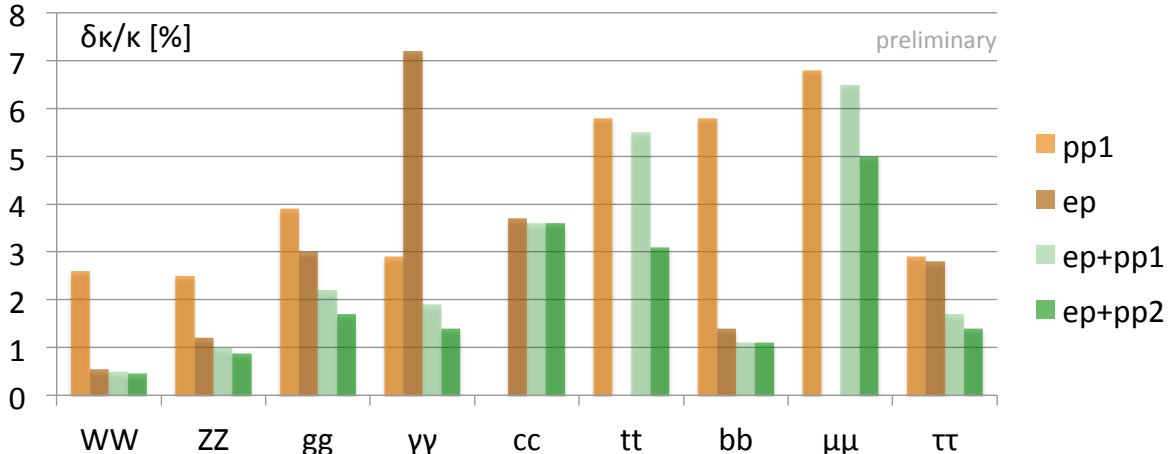


Figure 3: Determination of the κ scaling parameter uncertainties, in pp at HL-LHC, using CMS (S1, orange), ep with the LHeC (brown) and the LHeC jointly with CMS, for the conservative systematics (S1, light green) and the more challenging systematics (S2, green), see text. Empty bars, e.g. cc at LHC or $\mu\mu$ at LHeC indicate non (or badly) measurable decays.

in signal strength from the μ_b in the CC channel to κ_W . Sup-percent precision is obtained at the FCC-eh as is described in the FCC submission owing to a 5-fold enlarged H cross section, longer operation time and higher luminosity.

Currently the HL-LHC prospects for the signal strength measurements are coming out. Initially we have jointly analysed the CMS [26] and LHeC μ measurement expectations². A remarkable synergy of the pp and ep Higgs measurement potentials is observed when comparing the CMS, the LHeC and the joint pp & ep fit results displayed in Fig. 3. Comparing for each channel the pp expectation with the joint result, one observes major improvements in almost all channels. LHeC provides precision for bb , WW and ZZ and a second generation result for charm, while HL-LHC determines the rarer channels particularly well, illustrated here with the top and muon channels.

The HL-LHC results, for the non-rare channels, are systematics dominated. CMS presents [26] pp prospects for an estimated systematic level S_1 and also uses an anticipated level S_2 with half the S_1 systematics. The joint ep & pp analysis is here carried out for both S_1 and S_2 . A significant part of the systematics is the theoretical uncertainty, see [26]. LHeC will remove a substantial part of it, by providing external precision determinations of PDFs and α_s . One therefore may consider the ep & pp(S_2) result as the best possible estimate for the LHC Higgs facility at large. It is seen that, when combining pp and ep, the W , Z , gluon, photon, beauty and τ couplings may all be expected to be eventually known to about 1% from the enlarged LHC facility. The LHeC is recognised to indeed have the potential for **the LHC to become a laboratory for high precision Higgs physics**: The striking result is that the LHC, with prospects of measuring the width in pp to 5% [26], can provide SM Higgs measurements for the dominant channels as accurate as for example CLIC, and much more accurate for the rare channels than any e^+e^- collider, owing to the very large Higgs production cross section at the LHC. This high level of precision may as well be used to constrain EFT parameters which was beyond the κ framework analysis presented here.

The Higgs mechanism is regarded as a window to new physics and its exploration reaches much beyond establishing its SM decays though these may reveal new physics too when they depart from expectation. For the LHeC, summarised in [24], a wide range of **BSM Higgs physics topics** has been studied. These regard the ttH SM (to 15 (9)% with ep at HL (HE) LHC) and anomalous couplings, or the **Higgs \rightarrow invisible decay, a possible signature of Dark Matter** (to 5 (3)%). A large number of exotic Higgs LHeC prospect papers was published in recent years, as listed in [27]. For example, extended

²At the time of this draft the ATLAS results were not yet available but shall be considered as time permits.

241 gauge theories predict the **existence of further Higgs bosons**, such as a five-plet, singly charged Higgs
 242 H_5^\pm boson [28], which can be searched for at LHeC. Another example, difficult to study at the LHC, is an
 243 exotic Higgs decay mode into two new light scalars in a 4b final state which is well motivated in the Next to
 244 Minimal Supersymmetric Standard Model and extended Higgs sector models. The LHeC has energy larger
 245 than the e^+e^- 250 GeV Higgs facilities and cleanliness better than pp which explains its discovery potential
 246 and complementarity to other facilities.

247 1.5 Beyond the SM with ep and Empowering LHC Searches for New Physics

248 Because of the absence of color exchange between the electron and proton beams, ep colliders are ideally
 249 suited for a detailed study of electroweak interactions. The fact that leptons and quarks have the same elec-
 250 tric charge quantization and the same number of flavours suggests compositeness from common fundamental
 251 constituents. Through contact interactions, it is estimated that **compositeness scales $O(40)$ TeV can be**
 252 **probed at the LHeC**. Leptoquarks (LQ), predicted in technicolor theories, can be a direct manifestation
 253 of such compositeness. In ep collisions, LQ's can be produced in an s-channel resonance, the signature being
 254 a peak in the invariant mass of the outgoing ℓq system. The signal strength allows to infer the coupling
 255 constant λ between the electron and the quark. This is barely possible at the LHC, where the dominant
 256 pair production process via the strong interaction is insensitive to λ . If LQ's exist with mass below the
 257 center-of-mass energy of the collider, extreme sensitivity to λ can be achieved. Contrary to the LHC envi-
 258 ronment, at the LHeC many properties of the LQ's can be measured with good precision [1]. In addition,
 259 LQ-like signatures arise also in R-parity violating SUSY scenarios. If R-parity is violated, vertices are al-
 260 lowed that contain one SUSY particle only, with lepton or baryon number violation. The RPV couplings
 261 can be probed by e.g. multi-lepton and multijet signatures at the LHC. At the LHeC one can test anomalous
 262 e - d - t interactions $\lambda'_{131} < 0.03$ and also the product $\lambda'_{131}\lambda'_{i33}$ [29].

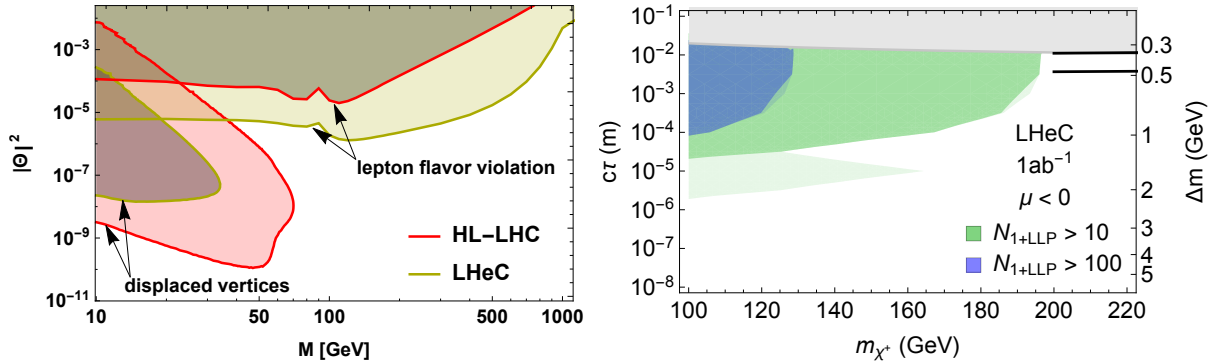


Figure 4: Left: Prospects for direct right-handed neutrino searches at the LHeC, first estimates for HL-LHC prospects for comparison, based on [30]. Right: Reach for long-lived Higgsinos in the mass (m_{χ^*}) - lifetime ($c\tau$) plane, compared to disappearing tracks at the HL-LHC [31], shown by the black lines. Light shading indicates the uncertainty in the predicted number of events due to different hadronization and LLP reconstruction assumptions. For details, see [32].

263 **Anomalous couplings** could be the first manifestations of electroweak interactions beyond the Stan-
 264 dard Model. Present constraints on anomalous triple vector boson couplings are dominated by LEP, but
 265 they are not free of assumptions. The WWZ and $WW\gamma$ vertices can be studied at LHeC in great detail. The
 266 process $e^-p \rightarrow e^- \mu^+ \nu j$ allows a sensitivity of about 10^{-3} via a shape analysis [33]. The **top quark FCNC**
 267 interactions, a good test of new physics because extremely suppressed in the SM, can be described in an
 268 effective theory, and two σ limits obtained translate into limits on the branching ratios $\text{Br}(t \rightarrow u\gamma)$ and
 269 $\text{Br}(t \rightarrow c\gamma)$ as small as 4×10^{-6} and 4×10^{-5} , respectively [34].

270 Models with **right handed sterile neutrinos** can explain the **generation of neutrino masses** via a
 271 low-scale seesaw mechanism. Mixing between the active and sterile neutrinos is strongly constrained by
 272 LEP, ruling out a discovery at HL-LHC. The search prospects for the low-scale seesaw neutrinos at ep are
 273 dominated by lepton-flavor violating processes, e.g. $e^-p \rightarrow \mu^- W + j$, and by displaced vertices for masses
 274 below m_W [30]. Jet substructure may help to distinguish the signal from the few SM backgrounds [35]. The
 275 search prospects for direct right-handed neutrinos with the LHC and HL LHC are shown in Fig. 4. It is

276 evident that this topic is one of the very promising BSM areas to be exploited at the LHeC which is the
 277 only means to directly discover low-scale seesaw neutrinos with masses above the energy threshold at the ee
 278 Higgs facilities.

279 Electron-proton colliders at high energy can explore significant regions of **supersymmetric parameter**
 280 space for which hadron colliders have low sensitivity. Higgsinos (χ) with masses $\mathcal{O}(100)$ GeV are moti-
 281 vated by natural SUSY theories which avoid large fine-tuning. In this regime, the low energy charginos
 282 (χ^\pm)/neutralinos(χ^0) are all Higgsino-like and their masses are nearly degenerate. The decays of the heavier
 283 χ^\pm to $W^\pm\chi^0$ yields final states without hard leptons, which makes these processes difficult to investigate at
 284 the LHC, where only the missing transverse momentum is observable. At the LHeC light χ^\pm (and χ^0) can
 285 be produced in pairs via the charged and neutral currents. A cut-based analysis of these processes at the
 286 LHeC, assuming prompt χ^\pm decays, yields discovery prospects for masses up to 120 GeV [36]. More strin-
 287 gent constraints can be placed if slepton masses are light but still higher than the chargino and neutralino
 288 masses. An analysis based on boost-decision tree and optimized for $\Delta m(\tilde{l}, \chi^0) = 10$ GeV scenarios show an
 289 increase in **discovery prospects with sensitivity for χ^\pm and χ^0 masses up to 230 GeV**.

290 Taking into account the displacement of the χ^\pm decay, and the visibility of tracks with $P_t \sim 0.1$ GeV al-
 291 lows LHeC tests of χ with masses up to 200 GeV [32], cf. Fig. 4 (right). Considering **non prompt decays of**
 292 **Higgsinos** thus significantly improves the discovery prospects compared to the prompt analysis. Long-
 293 lived-particles (LLPs) can result from the near **degeneracy of electroweakinos** or from many other BSM
 294 theories, yielding spectacular signals in collider experiments. For exotic Higgs decays into pairs of light LLP,
 295 the LHeC can test proper lifetimes that are smaller than $\sim \mu\text{m}$, which is significantly better than the reach
 296 of the LHC [32], where the sensitivity is rather to a mm.

297 1.6 The Case for Energy Frontier Electron-Ion Scattering

298 HERA missed to study electron-ion collisions. The LHeC will give access to a completely unexplored region
 299 of the kinematic x - Q^2 plane for nuclei, extended by 3 orders of magnitude when compared to fixed target
 300 DIS data, see Fig. 5 left. It therefore is expected to **thoroughly transform our present knowledge on**
 301 **parton structure in nuclei** providing also the chromodynamic base for the QGP and the ridge correlation
 302 phenomenon.

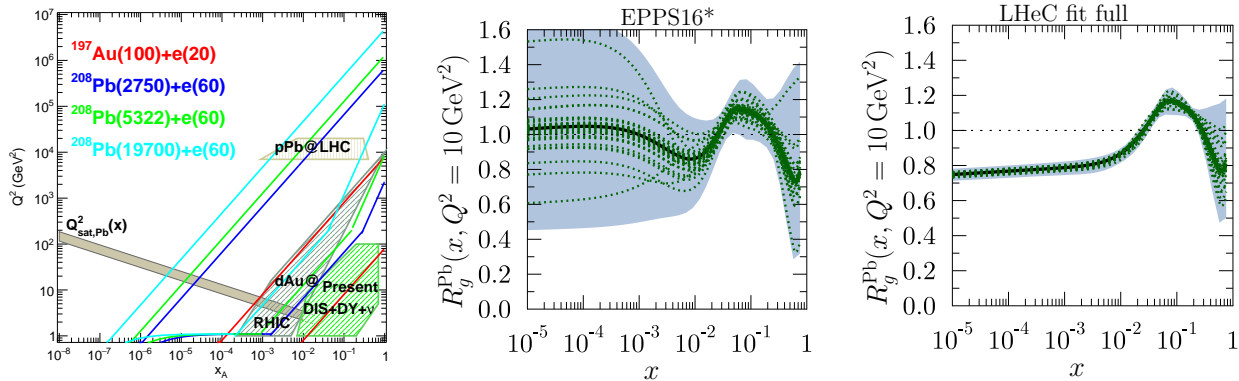


Figure 5: Left: x - Q^2 plane for future eA colliders also indicating the region covered by data used in present global fits and the estimated line of the saturation scale for Pb. Middle and right plots: Pb/p ratio of the gluon PDF in the modified EPPS16 analysis in [37], both for the present situation (middle) and including NC, CC and charm LHeC pseudo-data (right).

303 In the standard collinear framework used to compute particle production in hadronic collisions, parton
 304 distributions inside nuclei (nPDFs) are basically unknown for x below 10^{-2} where the DIS data base ends,
 305 as is illustrated in Fig. 5. The scarcity of data for any single nucleus makes it moreover mandatory to
 306 combine information on different ones. The LHeC eA data, with an expected luminosity of 10 fb^{-1} and their
 307 huge kinematic range provide a unique base, from NC, CC and heavy quark data, to **resolve the nuclear**
 308 **parton structure completely** [38] with very high precision as is illustrated in Fig. 5. This provides nuclear
 309 PDFs independently of proton PDFs and thus **unprecedented information on nuclear binding** as for

310 example flavour dependent shadowing effects.

311 **Diffractive nuclear parton densities have never been measured** and can be extracted at the LHeC
312 with similar precision to those inside the proton, against predictions of a much enhanced fraction of diffrac-
313 tion in eA as compared to ep. Exclusive LHeC vector meson production measurements are sensitive to the
314 **generalised parton densities inside nuclei** and thus to the transverse partonic structure. Separating
315 coherent diffraction, where the nucleus remains intact, from the incoherent case where it dissociates, will
316 characterise the fluctuations in the spatial parton distributions in protons and nuclei, a vital ingredient in
317 understanding hadronic collisions in both the soft and hard domains.

318 Being density effects, non-linear QCD phenomena are enhanced by both a decrease in x and by an increase
319 in the number of nucleons involved in the collision. At the LHeC, with its huge range in x for both ep and eA,
320 one expects to **discover or discard gluon saturation in the ep case** and cleanly disentangle it from nuclear
321 and also resummation effects. Fundamental studies on **nuclear effects on hadronisation and QCD**
322 **radiation** will be constrained by particle and jet production measurements studied in the LHeC CDR [1].

323 **The LHeC as an electron ion collider**, with its huge kinematic range and high precision, will all
324 have profound implications to our **understanding of all stages of heavy ion collisions** at high ener-
325 gies; the wave function of the colliding nuclei; the particle production mechanism; the initial spatial and
326 momentum distributions of produced partons prior to the emergence of a collective behaviour. This in-
327 cludes correlations such as those revealed by the **ridge phenomenon**, which may be explained both in
328 perturbative frameworks, like the Color Glass Condensate, or in non-perturbative ones, like the inelastic colli-
329 sion of gluonic flux tubes associated with the **QCD interactions responsible for quark confinement in**
330 **hadrons** and be ideally studied in electron-hadron scattering [39]. Furthermore, eA collisions will establish
331 a **baseline representing the normal (cold) nuclear medium**, relative to which the effects of the hot
332 dense medium can be contrasted for hard probes such as jets and quarkonia. The LHeC obviously is the
333 ideal machine for **revolutionising our understanding of nuclear structure and Chromodynamics**
334 and the natural complement and eventual successor of the HI programme at the LHC once that ends.

335 2 Overview on the LHeC Accelerator Design

336 The LHeC was basically designed in 2012, following extensive work and a final year of review prior to the
337 **publication of the Conceptual Design Report** [1]. The Higgs discovery set a higher luminosity goal
338 than foreseen in 2012 and the ERL frequency was finally set to 802 MHz, see [7]. The LHC performed
339 extremely well and technology, especially on SRF, made significant progress, as may be also seen from the
340 very successful first 802 MHz cavity fabrication and test, see the PERLE strategy paper [6]. The LHeC
341 work in recent years was mainly characterised, apart from adapting the physics to the findings of the LHC,
342 by studies in support of the 10^{34} luminosity goal, such as on beam-beam interactions or the IR design,
343 many still ongoing, by renewed investigations on the civil engineering and by the **foundation of an ERL**
344 **development facility, PERLE at Orsay**. The detector design and software developed considerably related
345 to physics requirements, as from Higgs final state reconstruction, and connected to the rapid develop-
346 ment of detector technology, especially by the HL LHC detector upgrades. The **current detector design**
347 and its possible implementation, like some of the here mentioned topics, are described in the Addendum [5].

348 **The core of the LHeC electron accelerator complex** consists of two superconducting 10 GeV linacs
349 with an RF frequency of 802 MHz that are connected by arcs in an energy recovery racetrack configuration.
350 see Fig. 6. The beam is injected at the beginning of the first linac and passes three times through either
351 linac, each time accelerated by about 10 GeV. Then it collides with the proton beam in the detector before it
352 passes another three times through the two linacs and is dumped. The timing for these passages is adjusted
353 such that the beam is decelerated and transfers its energy back into the cavities. Before the arcs, a beam
354 splitter is installed that distributes the beam into one of three beamlines in each arc, depending on its
355 energy. At the end of the arcs the beams are recombined. Special acceleration stations at the end of the arcs
356 compensate the energy loss due to synchrotron radiation. This configuration provides a colliding electron
357 beam with a very high power but because of the energy recovery the RF power for the linacs remains very
358 limited - it is only required to stabilise the RF amplitude and phase and compensate losses in the walls of

359 the cavities. This feature, combined with the dump at only injection energy, makes the ERL of the LHeC
 360 a genuinely *green* novel accelerator technique.

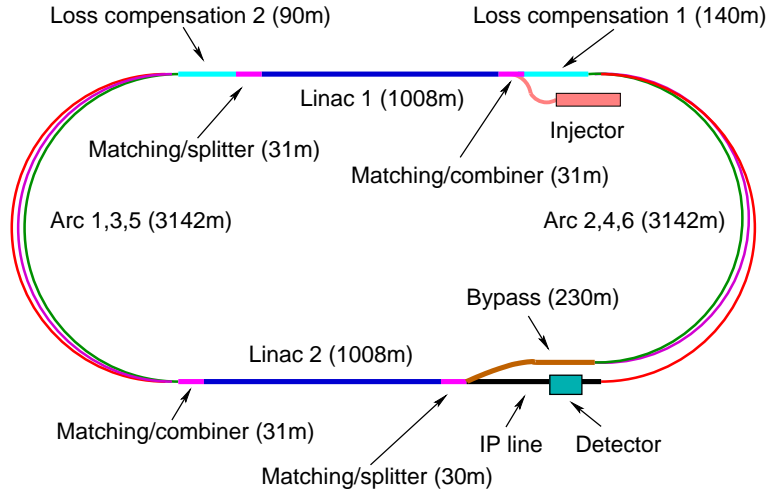


Figure 6: Schematic view of the default three-turn LHeC configuration with two oppositely positioned electron linacs of about 1 km length. Each linac accelerates the beam to 10 GeV and is made of about 45 cryomodules, housing four 5-cell 802 MHz cavities with a near to 20 MeV/m gradient. For 60 GeV, the ERL circumference is chosen to be 1/3 of that of the LHC.

360

361 The **key collective effects have been studied**. The optics design of the linacs optimises the beam
 362 stability over all six passages and in combination with the damping of transverse modes in the cavities
 363 ensures beam stability up to an electron beam bunch population of $4 \cdot 10^9$. Higher currents can be stabilised
 364 by further improving the damping. The electro-magnetic fields of the proton bunches strongly disrupt the
 365 colliding electron bunches. Careful choice of electron collision optics minimises the impact on the electron
 366 beam emittance and maximises luminosity. The electron beam bunch pattern is matched to the circulating
 367 proton beam such that each electron bunch collides with a proton bunch. This maximises luminosity and also
 368 avoids non-colliding electron bunches that due to the lack of disruption will have a much larger emittance
 369 after the collision. The impact of the electron beam on the proton beam emittance, especially in case of beam
 370 jitter, is acceptable as detailed studies showed. A potential instability that could be caused by trapping of
 371 ions in the beam can be mitigated by introducing gaps in the beam, which allow the ions to be removed;
 372 the charge of the remaining bunches is increased accordingly to maintain the luminosity.

373 This configuration, as detailed in [40], leads to **peak luminosity values of about $10^{34} \text{ cm}^{-2} \text{ s}^{-1}$** . This
 374 appears possible owing to the expectations of a high proton beam brightness and small emittance of the
 375 HL LHC proton beam. It furthermore requires electron currents of about 20 mA and eventually larger. For
 376 the interaction region design it calls for a β^* below 10 cm, which according to the **ongoing IR design**,
 377 sketched in the addendum [5] to this contribution, is indeed in reach. In a CERN official, joint paper on
 378 machine parameters of proposed future colliders at CERN, an **operation scenario** [41] was described for
 379 the LHeC with three phases of operation, following LS4, i.e. starting in the early thirties, which would
 380 permit to collect a luminosity of the order of 1 ab^{-1} with the LHeC, and of 2 ab^{-1} if the ERL was combined
 381 with HE LHC or the FCC, owing to modified parameters [40] and longer operation than will be possible
 382 with the LHC. In electron-lead scattering with the LHeC, an integrated luminosity of $O(10) \text{ fb}^{-1}$ may be
 383 collected. This may be compared with the total luminosity of 1 fb^{-1} delivered in ep over HERA's lifetime.
 384 Since, moreover, the cms energy of the LHeC in eA mode is much larger than in ep at HERA, one recognises
 385 the **extreme reach of the CERN EIC programme** using the ERL with the LHC.

386 The **Civil Engineering** (CE) of the LHeC was studied for the CDR [1]. It was re-visited in connection
 387 with the FCC conceptual design. The studies have assumed that the Interaction Region (IR) for LHeC will
 388 be at LHC Point 2, which currently houses the ALICE detector. The **location and size of the ERL**, for
 389 both the LHeC and the FCC-eh, are sketched in Fig. 7. For LHeC as far as possible, any surface facilities
 390 have been situated on existing CERN land. The physical positioning for the project has been developed
 391 based on the assumption that the maximum underground volume possible should be housed within the

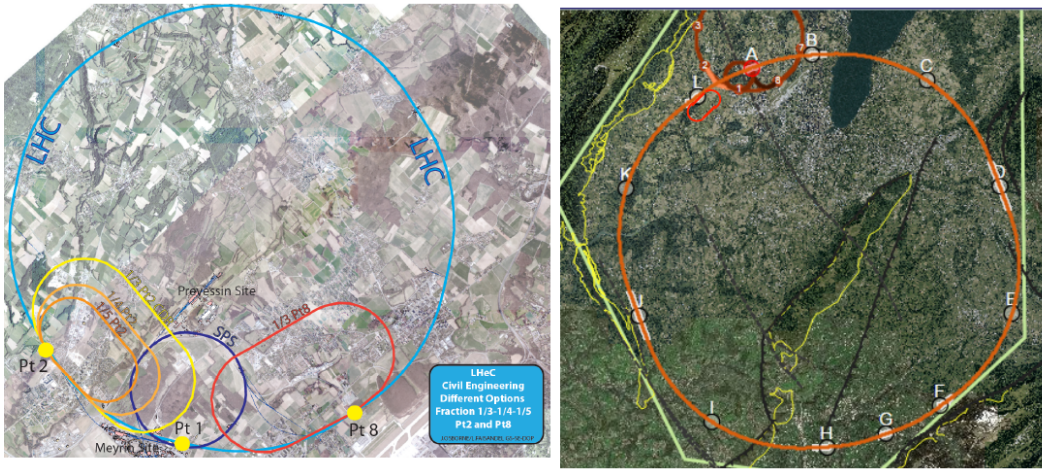


Figure 7: Possible locations of the ERL racetrack electron accelerator for the LHeC (left) and the FCC-he (right). The LHeC is shown to be tangential to Point 2 and Point 8. For Point 2 three sizes are drawn corresponding to a fraction of the LHC circumference of $1/3$ (outer, default with $E_e = 60$ GeV), $1/4$ (the size of the SPS, $E_e = 56$ GeV) and $1/5$ (most inner track, $E_e = 52$ GeV). Civil Engineering chose Point L as the position of the ERL at FCC, with two GPDs located at A and G.

392 Molasse Rock and should avoid as much as possible any known geological faults or environmentally sensi-
 393 tive areas. The shafts, one per linac, leading to any on-surface facilities have been positioned in the least
 394 populated areas, see the Addendum [5] for further details.

395

396 The LHeC CDR and its upgrade, the success of the DESY XFEL, the rapid international developments
 397 of SRF and ERL technology, all have revealed that complementing the LHC with a high energy ERL is a
 398 realistic, certainly challenging albeit unique opportunity. The time is 50 years after the discovery of quarks
 399 in ep scattering at Stanford. The LHeC linacs together are shorter than the 2 mile linac of SLAC. The LHeC
 400 is to complement the exploration of the TeV scale with the LHC and a possible future e^+e^- Higgs facility,
 401 as much as fixed target CERN muon and neutrino experiments accompanied the SppS and PETRA/PEP
 402 in the exploration of the $O(10)$ GeV scale, and HERA added crucial, independent information to Tevatron
 403 and LEP/SLC for the exploration of the Fermi scale. The SM was established over 5 decades through the
 404 interplay of energy frontier hadron-hadron, electron-positron and lepton-hadron experiments. Besides the
 405 discovery of quarks, deep inelastic scattering was instrumental in the discovery of asymptotic freedom, the
 406 clarification of the weak coupling of the electron and in the resolution of parton structure and with the
 407 discovery of gluon dominance at $x \leq 0.1$. The current key question is about physics beyond the standard
 408 gauge theory of electroweak and strong interactions. Using the singular hadron beams of the LHC for
 409 clarifying most pressing questions on the nature of the micro-universe, on the peculiarity of the Higgs mech-
 410 anism and for expanding the search for new physics, by realising an **"Electrons for LHC" programme**
 411 **is a most exciting option for the future of particle physics in the not too distant time.**

412 References

- 413 [1] J. L. Abelleira Fernandez et al. A Large Hadron Electron Collider at CERN: Report on the Physics and Design Concepts
 414 for Machine and Detector. *J. Phys.*, G39:075001, 2012.
- 415 [2] LHeC Collaboration. Exploring the Energy Frontier with Deep Inelastic Scattering at the LHC, An Update of the LHeC
 416 Conceptual Design Report, in preparation. 2019.
- 417 [3] Electrons for the LHC - LHeC/FCCh and PERLE Workshop, Orsay. <https://indico.cern.ch/event/698368/>. 2018.
- 418 [4] Zimmermann F. Aksakal H. Nergiz, Z. A High-Brilliance Angstrom-FEL based on the LHeC. *CERN-ACC-NOTE-2018-*
 419 *0061, ARIES 18-001*, 2018.
- 420 [5] LHeC Collaboration. Exploring the Energy Frontier with Deep Inelastic Scattering at the LHC, Addendum. 2018.
- 421 [6] PERLE Collaboration. A High Power Energy Recovery Facility for Europe, European PP strategy update. 2018.
- 422 [7] D. Angal-Kalinin et al. PERLE. Powerful Energy Recovery Linac for Experiments. CDR. *J. Phys.*, G45(6):065003, 2018.
- 423 [8] Chris Quigg. DIS and Beyond. *PoS*, DIS2013:034, 2013.

- 424 [9] Arthur M. Jaffe and Edward Witten. Quantum Yang-Mills Theory, 2000.
- 425 [10] S. Forte. LHeC: The Ultimate Factorization Machine, Talk at the LHeC Workshop at Chavannes-de-Bogis. 2012.
- 426 [11] Max Klein. Future Deep Inelastic Scattering with the LHeC, arXiv:1802.04317. 2018.
- 427 [12] S. Moch, B. Ruijl, T. Ueda, J. A. M. Vermaseren, and A. Vogt. Four-Loop Non-Singlet Splitting Functions in the Planar
428 Limit and Beyond. *JHEP*, 10:041, 2017.
- 429 [13] Richard D. Ball, Valerio Bertone, Marco Bonvini, Simone Marzani, Juan Rojo, and Luca Rottoli. Parton distributions
430 with small-x resummation: evidence for BFKL dynamics in HERA data. *Eur. Phys. J.*, C78(4):321, 2018.
- 431 [14] F. D. Aaron et al. Inclusive Deep Inelastic Scattering at High Q^2 with Longitudinally Polarised Lepton Beams at HERA.
432 *JHEP*, 09:061, 2012.
- 433 [15] Sukanta Dutta, Ashok Goyal, Mukesh Kumar, and Bruce Mellado. Measuring anomalous Wtb couplings at e^-p collider.
434 *Eur. Phys. J.*, C75(12):577, 2015.
- 435 [16] V. Andreev et al. Determination of electroweak parameters in polarised deep-inelastic scattering at HERA. *Eur. Phys. J.*,
436 C78(9):777, 2018.
- 437 [17] H Abramowicz et al. Combined QCD and electroweak analysis of HERA data. *Phys. Rev.*, D93(9):092002, 2016.
- 438 [18] Daniel Britzger and Max Klein. Precision electroweak physics at the LHeC and FCC-eh. *PoS*, DIS2017:105, 2018.
- 439 [19] ATLAS Collaboration. Prospect for a Measurement of the Weak Mixing Angle in pp to Z/y to ee events with ATLAS at
440 the HL-LHC. *ATL-PHYS-PUB-2018-037*, 2018.
- 441 [20] ATLAS Collaboration. Prospect for the Measurement of the W Boson Mass at the HL and HE-LHC. *ATL-PHYS-PUB-*
442 *2018-026*, 2018.
- 443 [21] Antonio O. Bouzas and F. Larios. Probing tt and ttZ couplings at the LHeC. *Phys. Rev.*, D88(9):094007, 2013.
- 444 [22] Hao Sun. Measuring the CKM matrix element V_{td} and V_{ts} at the electron proton colliders. *PoS*, DIS2018:167, 2018.
- 445 [23] I. Turk Cakir, A. Yilmaz, H. Denizli, A. Senol, H. Karadeniz, and O. Cakir. Probing the Anomalous FCNC Couplings at
446 Large Hadron Electron Collider. *Adv. High Energy Phys.*, 2017:1572053, 2017.
- 447 [24] Uta Klein. FCC-eh as a Higgs Facility. *Talk at FCC Week, Amsterdam*, 2018.
- 448 [25] Christoph Englert, Roman Kogler, Holger Schulz, and Michael Spannowsky. Higgs coupling measurements at the LHC.
449 *Eur. Phys. J.*, C76(7):393, 2016.
- 450 [26] CMS Collaboration. Sensitivity Projections for Higgs boson property measurements at the HL LHC. *CMS PAS FTR-18-*
451 *011*, 2018.
- 452 [27] Max Klein. From Quarks 1968 to Future DIS at CERN. *Opening Talk at the LHeC/FCCeh/PERLE Workshop on 'Electrons*
453 *for the LHC'*, 2018.
- 454 [28] Howard Georgi and Marie Machacek. Doubly Charged Higgs Bosons. *Nucl. Phys.*, B262:463–477, 1985.
- 455 [29] Hong-Tang Wei, Ren-You Zhang, Lei Guo, Liang Han, Wen-Gan Ma, Xiao-Peng Li, and Ting-Ting Wang. Probe R-parity
456 violating stop resonance at the LHeC. *JHEP*, 07:003, 2011. [Erratum: *JHEP*02,047(2013)].
- 457 [30] Stefan Antusch, Eros Cazzato, and Oliver Fischer. Sterile neutrino searches at future e^-e^+ , pp , and e^-p colliders. *Int. J.*
458 *Mod. Phys.*, A32(14):1750078, 2017.
- 459 [31] Rakhi Mahbubani, Pedro Schwaller, and Jose Zurita. Closing the window for compressed Dark Sectors with disappearing
460 charged tracks. *JHEP*, 06:119, 2017. [Erratum: *JHEP*10,061(2017)].
- 461 [32] David Curtin, Kaustubh Deshpande, Oliver Fischer, and Jos Zurita. New Physics Opportunities for Long-Lived Particles
462 at Electron-Proton Colliders. *JHEP*, 07:024, 2018.
- 463 [33] Ruibo Li, Xiao-Min Shen, Kai Wang, Tao Xu, Liangliang Zhang, and Guohuai Zhu. Probing anomalous $WW\gamma$ triple gauge
464 bosons coupling at the LHeC. *Phys. Rev.*, D97(7):075043, 2018.
- 465 [34] H. Denizli, A. Senol, A. Yilmaz, I. Turk Cakir, H. Karadeniz, and O. Cakir. Top quark FCNC couplings at future circular
466 hadron electron colliders. *Phys. Rev.*, D96(1):015024, 2017.
- 467 [35] Arindam Das, Sudip Jana, Sanjoy Mandal, and S. Nandi. Probing right handed neutrinos at the LHeC and lepton colliders
468 using fat jet signatures. 2018.
- 469 [36] Chengcheng Han, Ruibo Li, Ren-Qi Pan, and Kai Wang. Searching for the light Higgsinos in MSSM at the future e-p
470 colliders. 2018.
- 471 [37] Hannu Paukkunen. An update on nuclear PDFs at the LHeC. *PoS*, DIS2017:109, 2018.
- 472 [38] Max Klein. Nuclear Parton Distributions with the LHeC. *EPJ Web Conf.*, 112:03002, 2016.
- 473 [39] Stanislaw D. Glazek, Stanley J. Brodsky, Alfred S. Goldhaber, and Robert W. Brown. Ridge effect, azimuthal correlations,
474 and other novel features of gluonic string collisions in high energy photon-mediated reactions. *Phys. Rev.*, D97(11):114021,
475 2018.
- 476 [40] Jowett J. Klein M. Pellegrini D. Schulte D. Bruening, O. and F. Zimmermann. FCC-eh Baseline Parameters. *FCC-ACC-*
477 *RPT-0012*, 2017.
- 478 [41] Benedikt M. Bruening O. Jowett J. Rossi L. Schulte D. Stapnes S. Bordry, F. and F. Zimmermann. Machine Parameters
479 and Projected Luminosity Performance of Proposed Future Colliders at CERN. arXiv:1810.13011, 2018.